Mechanical Properties of Soft Magnetic (Fe0.76Si0.096B0.084P0.06)100-xCux (x = 0 and 0.1) Bulk Glassy Alloys

著者	Li Xue, Makino Akihiro, Yubuta Kunio, Kato Hidemi, Inoue Akihisa
journal or publication title	Materials Transactions
volume	50
number	6
page range	1286-1289
year	2009
URL	http://hdl.handle.net/10097/52255

Materials Transactions, Vol. 50, No. 6 (2009) pp. 1286 to 1289
Special Issue on Joining Technology for New Metallic Glasses and Inorganic Materials

Mechanical Properties of Soft Magnetic $(Fe_{0.76}Si_{0.096}B_{0.084}P_{0.06})_{100-x}Cu_x$ ($x = 0$ and 0.1) Bulk Glassy Alloys

Xue Li[1,*], Akihiro Makino[2], Kunio Yubuta[2], Hidemi Kato[2] and Akihisa Inoue[3]

[1]*Graduate School of Engineering, Tohoku University, Sendai 980-8579, Japan*
[2]*Institute for Materials Research, Tohoku University, Sendai 980-8577, Japan*
[3]*Tohoku University, Sendai 980-8577, Japan*

Fe-based bulk glassy alloys (BGAs) are known to have great potential for structural applications because of their high strength and relatively low material cost. However, their brittle nature hinders further applications. We have recently developed a new ductile $(Fe_{0.76}Si_{0.096}B_{0.084}P_{0.06})_{99.9}Cu_{0.1}$ BGA with a strength of 3.3 GPa and a large plastic strain of about 4% in compression. A well developed vein pattern on the fracture surface and highly-dense multiple shear bands on the surface of the specimen were observed. A large number of α-Fe like clusters (<10 nm) are found to disperse in the matrix glass. These clusters possibly act as nucleation sites for the α-Fe nanocrystallization in slipping shear bands dynamically. This results in development of the multiple shear bands causing highly improved plasticity in the $(Fe_{0.76}Si_{0.096}B_{0.084}P_{0.06})_{99.9}Cu_{0.1}$ BGA. [doi:10.2320/matertrans.ME200833]

(Received December 22, 2008; Accepted March 26, 2009; Published May 20, 2009)

Keywords: *iron-based bulk glassy alloy, plasticity, multiple shear bands, α-iron*

1. Introduction

Fe-based bulk glassy alloys (BGAs) with high strength, magnetic softness and relatively low material cost offer a great potential for a wide variety of applications.[1–6] However, the Fe-based BGAs which have been developed to date are lack in fracture toughness so that almost no plastic strain is obtained under uniaxial tensile or compressive deformations at room temperature. The ductility of the Fe-based BGAs is much inferior to that of non-ferrous BGAs.[4,7–9] This lack of plasticity followed by the catastrophic fracture limits the use of the BGAs in new structural applications. Therefore, great efforts have been made to improve the plastic deformation ability of many types of BGAs and the compressive ductility has been improved to a large extent by promoting multiple shear bands in Zr-,[10,11] Cu-,[12–14] Ni-,[15,16] Ti-,[17,18] Mg-,[19] and Pd-based[20] BGA composites containing second dendrite or particle phases, or fine pore phase in the BGA matrices. However, improvements in ductility of the Fe-based BGAs, which have higher strength than the non-ferrous alloys, have not been achieved yet.

We recently have reported that the addition of P significantly increases the glass-forming ability (GFA) of the ordinary melt-spun Fe-Si-B amorphous alloys, whose critical glass forming size is less than 100 µm in thickness. A $Fe_{76}Si_9B_{10}P_5$ alloy, consisting only of iron metal and metalloid elements, is found to exhibit high GFA of 2.5 mm in the critical glass-forming diameter by the conventional copper-mold casting technique and high yielding stress of 3.3 GPa, followed by a plastic deformation of 0.7% in compression, which is rather larger than the Fe-based BGAs (∼3 GPa[7,8]). The iron-rich Fe-metalloid BGAs also show a high magnetization of 1.51 T, low coercivity of 0.8 A/m, and relatively low material cost compared to those previously reported for Fe-based BGAs including other metal elements.[21)]

We have investigated the effect of adding small amounts of copper, which has a large negative mixing enthalpy with Fe and no-solubility into Fe in solid,[22] on the structure and mechanical properties in the Fe-metalloid BGAs. In this paper, we intend to demonstrate excellent mechanical properties of a newly developed ductile $(Fe_{0.76}Si_{0.096}B_{0.084}P_{0.06})_{99.9}Cu_{0.1}$ BGA having high magnetization (1.5 T) as well as low coercivity (1.9 A/m).

2. Experimental Procedure

$(Fe_{0.76}Si_{0.096}B_{0.084}P_{0.06})_{100-x}Cu_x$ ($x = 0$ and 0.1 at%) alloy ingots were produced by induction melting mixtures of pure Fe (99.998 mass%), Si (99.99 mass%), B (99.9 mass%), Cu (99.99 mass%) and pre-alloyed Fe-26.5 mass% P ingots in a high purity argon atmosphere. Their compositions are nominally expressed in atomic percentage. From the master alloys, ribbons and cylindrical rods were produced by the melt-spinning and copper mold casting techniques, respectively.

The structure of the specimens was examined by the X-ray diffractometry (XRD) with Cu-Kα radiation, and transmission electron microscopy (TEM). Thermal stability associated with the onset temperatures for the glass transition (T_g) and crystallization (T_x) of the glassy samples was evaluated by differential scanning calorimetry (DSC) at a heating rate of 0.67 K/s. Magnetic properties, such as saturation magnetization (M) and coercive force (H_c), were measured by a vibrating sample magnetometer (VSM) under an applied field of 400 kA/m and a B–H loop tracer under a field of 800 A/m, respectively. The mechanical properties of yield stress, fracture stress and compressive plastic strain were measured by an Instron testing machine. The gauge dimensions of the testing sample were 1 mm (circumferentially) and 3 mm (longitudinally), and the strain rate was set to $5 \times 10^{-4}\,s^{-1}$. The deformation and fracture behaviors were examined by scanning electron microscopy (SEM).

*Corresponding author, E-mail: lixue@imr.tohoku.ac.jp

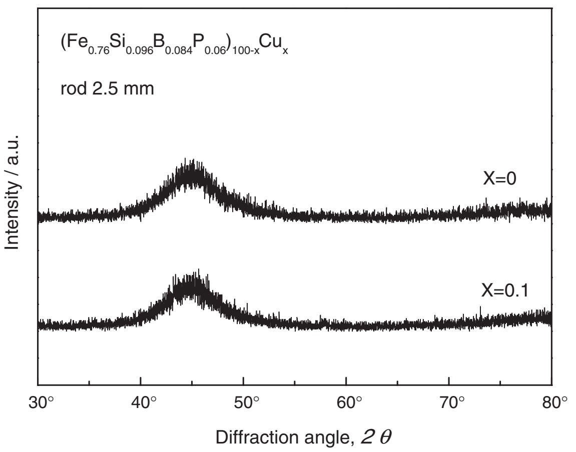

Fig. 1 XRD patterns of $(Fe_{0.76}Si_{0.096}B_{0.084}P_{0.06})_{100-x}Cu_x$ ($x = 0$ and 0.1) bulk glassy alloy rods.

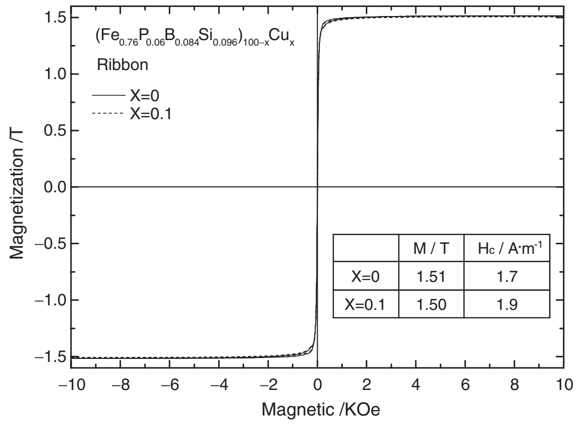

Fig. 3 *B–H* loop traces of glassy alloy ribbons $(Fe_{0.76}Si_{0.096}B_{0.084}P_{0.06})_{100-x}Cu_x$ ($x = 0$ and 0.1).

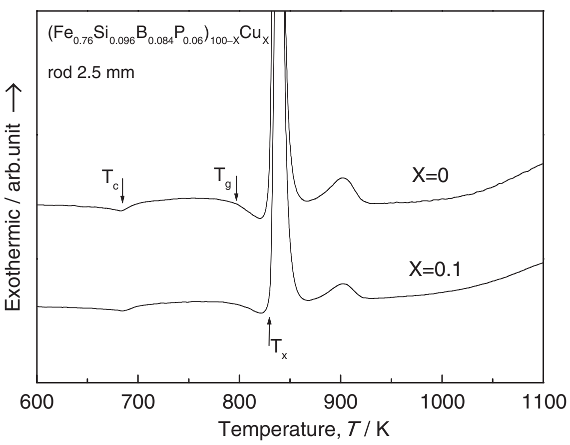

Fig. 2 DSC traces of $(Fe_{0.76}Si_{0.096}B_{0.084}P_{0.06})_{100-x}Cu_x$ ($x = 0$ and 0.1) bulk glassy alloy rods at a heating rate of 0.67 K/s.

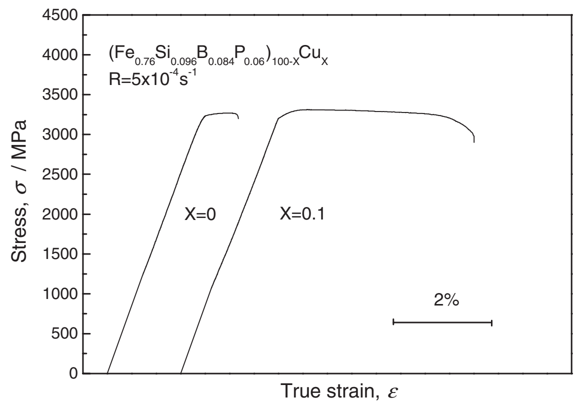

Fig. 4 True compressive stress-strain curves of as-cast $(Fe_{0.76}Si_{0.096}B_{0.084}P_{0.06})_{100-x}Cu_x$ ($x = 0$ and 0.1) glassy rod specimens at a strain rate of $5 \times 10^{-4}\,s^{-1}$.

3. Results and Discussion

The as-cast $(Fe_{0.76}Si_{0.096}B_{0.084}P_{0.06})_{100-x}Cu_x$ ($x = 0$ and 0.1) BGAs were confirmed to be of single glassy phase by the XRD analysis as shown in Fig. 1. These alloys have a wide super-cooled liquid region, one of the parameters for expressing GFA defined by the temperature interval between the onset temperatures of the glass transition and crystallization (ΔT_x), of 48 and 46 K at a heating rate of 0.67 K/s, respectively as shown in Fig. 2. These BGAs exhibits good soft-magnetic properties as shown in Fig. 3. The saturation magnetization does not change so much from 1.51 T for the alloy without Cu to 1.50 T for the 0.1 at% Cu-added alloy. The alloy ribbons are found to have low H_c of 1.7–1.9 A/m.

We further measured the mechanical properties of these Fe-based BGA specimens, whose dimensions are 1.5 mm in diameter and 3 mm long, by compression testing. Figure 4 shows the compressive true stress-strain curves for $(Fe_{0.76}Si_{0.096}B_{0.084}P_{0.06})_{100-x}Cu_x$ ($x = 0$ and 0.1) BGAs. The yield stress, defined in this work by a deviation of 0.2% from the linear relation, and the elastic limit are 3.25 GPa and ~1.9%, respectively, for both alloys. After yielding, the alloys exhibit a maximum stress of 3.3 GPa then stress gradually decreases with further increase in strain. Plastic strain is ~0.7% for the alloy without Cu, which is an average of three samples (0.5–0.9%). On the contrary, it increases significantly up to ~4% for the 0.1% Cu-added alloy, which is the best one among five samples (2.5–4%). The small amount Cu-addition results in highly improvement on plasticity in the Fe-based BMGs, which has been well known to be brittle in nature.[8] As shown in the inset of Fig. 4, the distinguishable serrated characteristics attributed to the formation of shear bands are not clearly observed. The relative smooth flow behavior should be closely related to the highly-dense multiple shear bands, which is shown in Fig. 6.

Figure 5 shows SEM images revealing that the Cu-added glassy rod has the vein pattern on a fracture surface and multiple shear bands on specimen surface while the Cu-free one does not. The fracture surface exhibits a well developed vein pattern, which is usually observed in the non-ferrous ductile BGAs. Moreover, density of multiple shear bands is high. The spacing between the shear bands is as small as 10–50 µm, which should be closely related to the absence of the serrated characteristics in the stress-strain curve and a large plastic deformation for the Cu-added alloy shown in Fig. 4. A result showing relatively large plastic deformation has been reported recently for Fe-based BGAs, and the large plastic deformation was attributed to the formation of the well

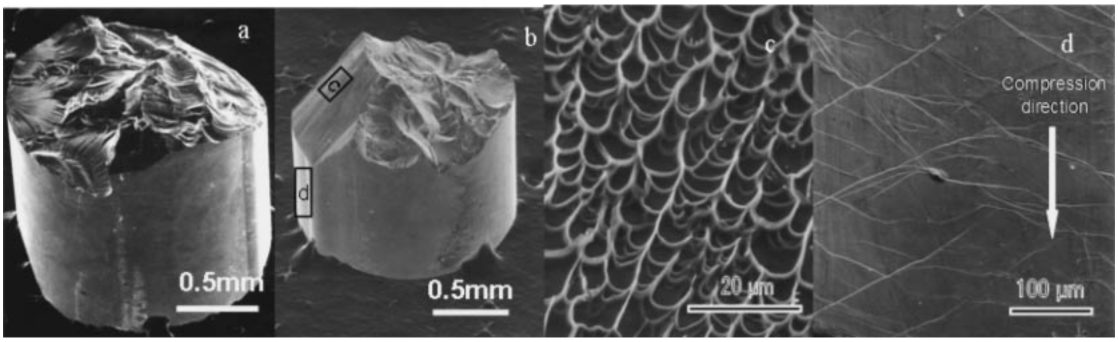

Fig. 5 The SEM images of (a) $Fe_{76}Si_{9.6}B_{8.4}P_6$ fractured specimen; (b) $(Fe_{0.76}Si_{0.096}B_{0.084}P_{0.06})_{99.9}Cu_{0.1}$ fractured specimen; (c) the vein pattern on the fracture surface taken in (c) region indicated in (b); and (d) the multiple shear bands on the specimen surface taken in (d) region indicated in (b).

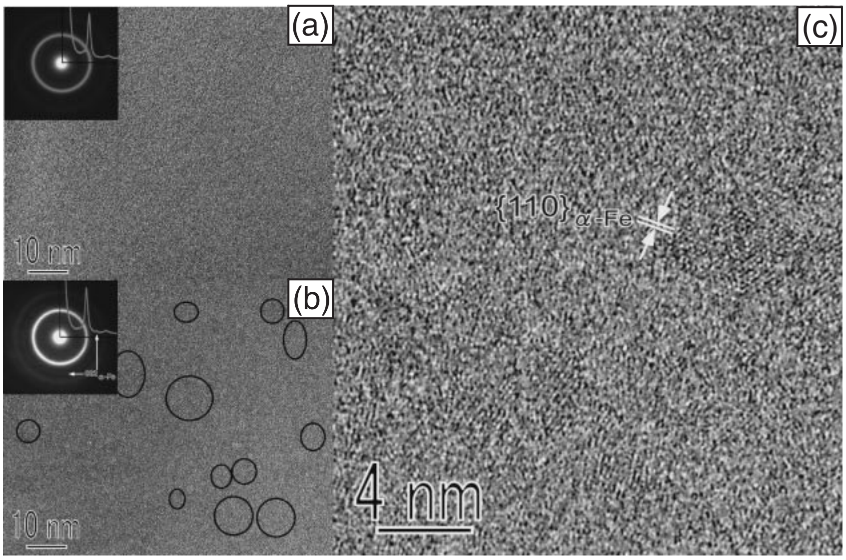

Fig. 6 High-resolution TEM images and the corresponding SAED patterns with the intensity profiles for (a) as-cast $Fe_{76}Si_{9.6}B_{8.4}P_6$ and (b) as-cast $(Fe_{0.76}Si_{0.096}B_{0.084}P_{0.06})_{99.9}Cu_{0.1}$ BGAs. An enlarged image of (b) is also shown in (c).

developed vein pattern and the distinguishable highly-dense multiple shear bands.[23] In general, plastic deformation of glassy alloys is highly localized into shear bands, followed by rapid slipping of these shear bands and a sudden fracture. Therefore, the highly-dense multiple shear bands result in large plastic deformation.[24] This fracture behavior with good ductility has not been observed for Fe-based BGAs to date.

The origin of the unusual ductile fracture behavior of the Cu-added Fe-based BGA is important to be solved. Figures 6(a) and 6(b) show high-resolution TEM images and the corresponding selected area electron diffraction (SAED) patterns taken from the cross-section of the as-cast rod specimens with and without Cu element, respectively. The dispersion of a large number of α-Fe like clusters with diameter less than 10 nm in the glassy matrix phase was observed in the TEM image, and a (200) peak from α-Fe was found in the SAED pattern for the Cu-added alloy (Fig. 6(b)). An enlarged image of Fig. 6(b) is shown in Fig. 6(c). The bars and arrows indicate the $\{110\}$ lattice fringes of an α-Fe phase. The alloy without Cu exhibiting the low plastic deformation of 0.7% shows a completely monolithic glassy structure. Therefore, the clusters observed in the alloy with Cu exhibiting the high plasticity of about 4%, should be related to the large plasticity.

We have already reported that the simultaneous addition of P and Cu to the ordinal Fe-Nb-B amorphous alloy introduces structural inhomogeneity, such as nano-scaled α-Fe clusters in the amorphous matrix, which might act as a nucleation site for α-Fe phase crystallization. A nanocrystalline structure with narrower grain size distribution can be obtained after appropriate annealing.[25] As the mixing enthalpy between Fe and Cu is positive, a repulsive interaction should exist between Fe and Cu atoms in the alloys. On the other hand, attractive interactions should exist between Cu and P, and P and Fe. Therefore, the as-cast structure possibly consists of two phases; the major part with an Fe-metalloid based glassy phase, and the minor part with a Cu-rich phase, which is considered to become the crystalline phase. A rapid increase in temperature has been reported in the vicinity of the highly stressed shear-slipping region.[26] Considering this, the cluster might act as a nucleation site of α-Fe nanocrystallization possibly taking place dynamically during the compressive test. For a composite structure with a glassy and ductile crystalline phases, the shear bands must interact with the microscale ductile crystalline phase during the propagation of shear bands under loading and their propagation direction have to be deflected, thus resulting in a shear band branching. At the same time, the shear bands are also blocked or branched by other intersected shear bands. Thus, the formation of a large number of the branching shear bands leads to a large increase in the macroscopic plasticity. Therefore, stress-induced dynamic nanocrystallization during compression is considered as a reason for the large plasticity of the Cu-added Fe-based BGA. This result will open the way for structural applications of high-strength Fe-based BGAs. Moreover, this Fe-based BGA composed of familiar and low-priced elements is of great advantage for engineering industry, and thus significantly improves the conservation of natural resources and environment.

4. Conclusions

(1) $(Fe_{0.76}Si_{0.096}B_{0.084}P_{0.06})_{100-x}Cu_x$ ($x = 0$ and 0.1) alloys show the high glass-forming ability with the critical glass forming diameter up to 2.5 mm by the copper mold casting method.
(2) Cu-added Fe-metalloid bulk glassy alloy, $(Fe_{0.76}Si_{0.096}B_{0.084}P_{0.06})_{99.9}Cu_{0.1}$, exhibits excellent mechanical properties: maximum stress of 3.3 GPa; Young's modulus of 163 GPa and a large plastic deformation of about 4% in compression.
(3) The well-developed vein pattern on the fracture surface and highly dense multiple shear bands on the surface of the rod specimen near the fracture surface are observed in $(Fe_{0.76}Si_{0.096}B_{0.084}P_{0.06})_{99.9}Cu_{0.1}$ alloy.
(4) A large number of α-Fe like clusters (less than 10 nm) are found to disperse in a glassy matrix. These clusters are considered to act as nucleation sites for the dynamic nanocrystallization of the α-Fe phase in the shear bands. This might result in developing the high-dense multiple shear bands which are responsible for the macroscopic compressive plasticity of the alloy.

Acknowledgement

One of the authors (XL) wishes to acknowledge the financial support of the Global COE Program "Materials Integration (International Center of Education and Research), Tohoku University", MEXT, Japan.

REFERENCES

1) A. Inoue: Acta Mater. **48** (2000) 279–306.
2) A. Inoue and B. L. Shen: Mater. Trans. **43** (2002) 766–769.
3) B. L. Shen, M. Akiba and A. Inoue: J. Appl. Phys. **100** (2006) 043523.
4) M. Stoica, J. Eckert, S. Roth, Z. F. Zhang, L. Schultz and W. H. Wang: Intermetallics **13** (2005) 764–769.
5) B. L. Shen, A. Inoue and C. T. Chang: Appl. Phys. Lett. **85** (2004) 4911–4913.
6) S. J. Pang, T. Zhang, K. Asami and A. Inoue: Acta Mater. **50** (2002) 489–497.
7) A. Inoue, B. L. Shen, A. R. Yavari and A. L. Greer: J. Mater. Res. **18** (2003) 1487–1492.
8) X. J. Gu, S. J. Poon and G. J. Shiflet: J. Mater. Res. **22** (2007) 344–351.
9) K. Amiya, A. Urata, N. Nishiyama and A. Inoue: Mater. Trans. **45** (2004) 1214–1218.
10) C. Fan, R. T. Ott and T. C. Hufnagel: Appl. Phys. Lett. **81** (2002) 1020–1022.
11) C. Fan and A. Inoue: Appl. Phys. Lett. **77** (2000) 46–48.
12) C. L. Qin, W. Zhang, K. Asami, H. Kimura, X. M. Wang and A. Inoue: Acta Mater. **54** (2006) 3713–3719.
13) J. Das, M. B. Tang, K. B. Kim, R. Theissmann, F. Baier, W. H. Wang and J. Eckert: Phys. Rev. Lett. **94** (2005) 205501.
14) K. B. Kim, J. Das, F. Baier, M. B. Tang, W. H. Wang and J. Eckert: Appl. Phys. Lett. **88** (2006) 051911.
15) J. K. Lee, H. J. Kim, T. S. Kim, Y. C. Kim and J. C. Bae: J. Alloy. Compd. **434** (2007) 336–339.
16) M. H. Lee, J. Y. Lee, D. H. Bae, W. T. Kim, D. J. Sordelet and D. H. Kim: Intermetallics **12** (2004) 1133–1137.
17) H. Guo, E. Jurgen, L. Wolfgang and S. Ludwig: Nat. Mater. **2** (2003) 33–37.
18) F. X. Qin, X. M. Wang and A. Inoue: Intermetallics **15** (2007) 1337–1342.
19) J. S. C. Jang and J. Y. Ciou: Appl. Phys. Lett. **92** (2008) 011930.
20) T. Wada, A. Inoue and A. L. Greer: Appl. Phys. Lett. **86** (2005) 251907.
21) A. Makino, T. Kubota, C. T. Chang, M. Makabe and A. Inoue: Mater. Trans. **48** (2007) 3024–3027.
22) O. Kubaschewski, J. F. Smith and D. M. Bailey: Z. Metallkd. **68** (1977) 495–499.
23) T. Zhang, F. G. Liu, S. G. Pang and R. Li: Mater. Trans. **48** (2007) 1157–1160.
24) Y. H. Liu, G. Wang, R. J. Wang, D. Q. Zhao, M. X. Pan and W. H. Wang: Science **315** (2007) 1385–1388.
25) A. Makino, M. Bingo, T. Bitoh, K. Yubuta and A. Inoue: J. Appl. Phys. **101** (2007) 09N117.
26) M. W. Chen, A. Inoue, W. Zhang and T. Sakurai: Phys. Rev. Lett. **96** (2006) 245502.